Surface area modelling for the craters and ejecta produced during 4.1-3.8 Ga: implications for the Late Heavy Bombardment of the Moon

López-Bautista, V. H.[1], Cordero-Tercero, G.[2], Gomez-Rubio, C.[3]

[1] https://orcid.org/0009-0005-1376-9083

[2] https://orcid.org/0000-0001-8135-9792

[3] https://orcid.org/0000-0002-2502-8101

1. Universidad Nacional Autónoma de México. Escuela Nacional de Estudios Superiores Morelia. Morelia, Michoacán, México.

2. Universidad Nacional Autónoma de México. Instituto de Geofísica, Sección de Riesgos Espaciales. Ciudad de México, México.

3. Universidad Nacional Autónoma de México. Instituto de Geografía, Laboratorio de Análisis Geoespacial. Ciudad de México, México.

RESUMEN:

En la década de 1970, un grupo de investigadores estimó la edad de las rocas lunares traídas por la misión Apollo, encontrando muy pocas de ellas con edades anteriores a 4.2 Ga. Para explicar esto, se propuso que en las etapas tempranas, tras la formación del sistema solar, hubo un aumento en la tasa de impactos de tal manera que se destruyeron las rocas más antiguas. Este evento hipotético fue llamado originalmente “Cataclismo lunar terminal” y renombrado posteriormente como “Gran Bombardeo tardío” (LHB, Late Heavy Bombardment, por sus siglas en inglés). Con el tiempo se han dado argumentos y contraargumentos para sostener, o no, esta hipótesis. En este trabajo, se empleó un modelo para estimar el área cubierta por los cráteres de impacto y sus eyectas continuas considerando que la tasa de impacto decae exponencialmente entre 4.1 y 3.8 Ga sin la presencia de un aumento súbito en la producción de cráteres, es decir, sin considerar un escenario tipo LHB. Para estimar el área afectada por la formación de un cráter de impacto, consideramos tres escenarios en los cuales las extensiones de sus eyectas fueron de 0.5 Rc, 1 Rc y 1.5 Rc, donde Rc es el radio del cráter. El área de la superficie de la Luna cubierta en cada caso fue de 83 %, 95.7 % y 99.2 %, respectivamente. Esto indica que un LHB no es necesario para explicar la carencia de rocas con edades mayores a 4.2 Ga. Si bien estos resultados no son por sí mismos suficientes para rechazar la hipótesis del LHB, contribuyen en la discusión de este tema.

Palabras clave: Gran Bombardeo Tardío, Hipótesis del muro de piedra

ABSTRACT:

The lack of lunar sample rock ages before 4.2 Ga, found by some authors, was explained because of a more intense bombardment than the expected for that time. This hypothetical event was initially named the “Terminal Lunar Cataclysm” and later renamed as the Late Heavy Bombardment (LHB). Over time, arguments and counterarguments have been given to support or not this hypothesis. In this work, a model was used to estimate the covered area by impact craters and their ejecta considering an exponentially declining impact rate for the period between 4.2 and 3.8 Ga without taking into account an LHB-type event. To estimate the area affected by the formation of an impact crater, we considered three scenarios in which the extent of the ejecta was 0.5 Rc, 1 Rc, and 1.5 Rc, where Rc is the radius of the crater. The area of the Moon's surface covered in each case was 83%, 95.7%, and 99.2%, respectively.This indicates that an LHB is not needed to explain the lack of lunar rocks

with ages older than 4.2 Ga. Even though these results are not enough, by themselves, to refute the LHB, they can contribute to the discussion around it.

Keywords: Late Heavy Bombardment, Stone wall hypothesis

1. Introduction

The Late Heavy Bombardment (LHB from now on) is a term that has been used in diverse ways by some authors (e.g. Frey, 2016; Lowe & Byerly, 2018; Morbidelli et al., 2012, 2018). In recent years, the LHB refers mainly to either a period at the end of terrestrial planet formation in which the impact rate declined slowly or an abrupt and short duration period when a sudden increase in the impact rate occurred, as a cataclysmic event (Cartwright et al. 2022). In this study, we consider the LHB as the second one, and it is defined as an important rise in the impact rates on the surface of the Moon 4.2 Ga followed by a decrease by 3.8 Ga; independently from the origin of the impactors or the mechanism involved in such a rise of the impact rates.

Even though the LHB is still under discussion, in some scenarios it is commonly referred to as a fact (Mainly in lectures regarding the formation of the solar system). The “stone wall” effect hypothesis is an important counterargument to the LHB and suggests that the “natural” impact flux in the Moon’s surface must have been responsible for the lack of rocks older than 4.2 Ga, “evidence” used to propose the LHB (Tera et al., 1974). In this work, the “stone wall” hypothesis was modelled employing a method to assess the surface area covered by impacts during the LHB temporalities under a simple declining impact flux.

1.1. Arguments in favour

1.1.1. Geochemical arguments

The first proposal leading to the Late Heavy Bombardment hypothesis was the then-called “Terminal Lunar Cataclysm” (Tera et al., 1974), to explain why the radiometric dates of the Apollo and Luna mission’s samples presented a concentration at around 3.9 Ga and a lack of older rocks. Later, a similar finding was described by Cohen (2000) and Cohen et al. (2000) from 40Ar-39Ar dates on lunar meteorites.

An abstract presented by Day & Neal (2024) describes relationships between several impactors and lunar impact melt samples suggesting that they formed on a short time span consistent with that of the LHB.

1.1.2. Dynamical arguments

A year after the proposal of the LHB, Monte-Carlo simulations showed that it is dynamically possible for orbital disturbances to have occurred in the early solar system so the impact flux in the inner solar system would have risen at ~3.9 Ga (Wetherill, 1975).

Gomes et al. (2005) proposed the delay of a mean-motion resonance (MMR) of 1:2, between the orbits of Jupiter and Saturn, so that the resulting instability would have promoted the LHB. Such a model, better known as the Nice model, considers the entrance of material coming from the outer regions of the solar system and the dominance of cometary impactors.

According to Kring and Cohen (2002), asteroidal impacts may have dominated during the LHB temporalities. This led to the proposal of an extended asteroid belt (E-belt) to take into account a larger number of asteroids as the impactor population, according to dynamic models. The resulting model, the Sawtooth model, suggests that the LHB timeline has a “sawtooth-like” profile with an uptick at ~4.1 Ga (Morbidelli et al., 2012). This profile is in agreement with: a) the lack of rocks with ages older than

~4.2 Ga (Tera et al., 1974), b) the impact records on icy bodies originated from the instability of the cometary orbits according to the model described in Gomes et al. (2005), and c) the geochemical constraints for ages older to ~4.1 Ga (studies of platinum-group elements on lunar samples from Cohen, 2000, and Cohen et al., 2000 and Kring & Cohen 2002). This model is also considered as a refined version of the Nice model. Throughout the years, the model has undergone a series of modifications resulting in the derivation of new Nice-like models describing similar migrations and instabilities of the Gas Giants (Hartmann, 2019).

1.1.3. Other arguments

Some other arguments include: 1) Based on LOLA data, Frey et al. (2016) carried out a correlation between the topography and the Bouguer anomaly of probable quasi-circular structures found on the lunar surface. According to this correlation, older basins have lower relief and Bouguer gravity contrasts than younger basins implying that the first basins formed under different crustal conditions, i.e., when deformation in the crust due to basin formation was more easily compensated. According to this study, there were actually two periods of intense bombardment, an Early Heavy Bombardment about 4.2 Ga ago and the LHB about 4 Ga ago, the former being more intense than the latter. 2) The inference of big impacts on Earth's surface from extra-terrestrial Ir and Cr abundances measured in spherulites from 8 layers of the Barberton's Green Rock Belt, resulting in the proposal of two heavy bombardment periods in the solar system: the first between 3.47 and 3.22 Ga and the second one between 2.63 and 2.49 Ga (Lowe & Byerly, 2018). This could be weak evidence that, throughout its history, Earth could have had episodes with an increase in the impact flux, so this could have also happened 4.2 Ga ago, and 3) the finding of stellar systems that appear to be experiencing a LHB of their own, such as η Corvi and KIC 8462852, where, from Near-Infrared studies, a copious amount of dust was detected in the Kuiper Belts of these systems which were interpreted to be dynamically excited. The explanation is that a planetary migration triggered collisions that produced the exceeding dust (Lisse et al., 2012, 2016).

Fournier et al. (2022), using a molecular clock, show that the last common ancestor of Bacteria existed shortly after 3.8 Ga. According to this result, they commented that this is consistent with the LHB impact bottleneck hypothesis in that life could only emerge after the impact rate decreases enough to avoid sterilisation by huge impacts. This approach does not permit to say how the impact rate was before 3.8 Ga.

1.2. Arguments against

1.2.1. Dynamical arguments

In the context of dynamics and solar system orbital evolution, the LHB seems to no longer be a variable to consider (Raymond, 2024). In the field, the discussion has now been shifted towards the timing of a Giant Planet instability like the one on the Nice model. The trend so far favours the early instability scenario ($t<100$) rather than the late instability one (consistent and/or similar to the Nice model and the LHB) (e.g. Clement et al. 2023, Nesvorny et al. 2023, Izidoro et al. 2024). However, in the planet formation context it is considered to still be relevant or at least a factor to be considered (Mordasini & Burn, 2024).

1.2.2. Geochemical arguments

As time went by, an open system behaviour was found on most of the Ar-Ar plateau ages from Apollo missions' samples (Boehnke & Harrison, 2016; Harrison et al., 2018). This represents a problem for the reliability of the ages from which the LHB was inferred. These studies also invoked and tested the effect described in Hartung (1974) and later cited by Wetherill (1975) where the age distributions used to describe the LHB could be reproduced taking into account the production and destruction from a "natural" declining impact rate.

The use of Ru and Mo isotopes has been used to distinguish the origin of the impactors related to two moon meteorites and three melt samples from Apollo 16; the possible origins being nebular carbonaceous or non-carbonaceous reservoirs; representing outer and inner regions of the protoplanetary disk (regarding Jupiter's orbit), respectively. These works have shown that all the impactors studied come from the inner solar system and that it is unlikely that an LHB had occurred as the result of an instability of the protoplanetary disk. In such a case, a part of the impactor population should have originated from regions outside of Jupiter's orbit. They state that in case a LHB could have occurred, this would have been produced by impactors late to accrete (Worsham & Kleine, 2020, 2021).

Melt ages have also been used to compare different scenarios: the tail-end (Neukum et al. 2001), the sawtooth model (Morbidelli et al. 2012), and the terminal cataclysm (being the tail-end scenario but with a peak at 3.9 Ga as described in Tera et al. 1974). As a result of this comparison, Liu et al. (2023) conclude that the least consistent model with their simulations and melt ages is the terminal cataclysm scenario and the most favourable one is the tail-end one.

In the field of geochemistry there are still publications showing more cases of planetary materials presenting no evidence for a LHB in the inner solar system (e.g. Walton et al. 2023, White et al. 2024).

1.2.3. Geophysical arguments

Baldwin (2006) analyses three previous interpretations, based on Apollo missions' data, which led to the formulation of the Terminal Lunar Cataclysm. The first of them being that there were no rocks with ages much older than the Imbrium basin. However, Baldwin notes that Imbrium's ejecta is abundant enough in the regions of the six landing sites of the Apollo missions, and that most of the samples show Imbrium's age. The second interpretation is that the samples from Apollo 16 were related to the formation of the Nectaris basin, simply because of its landing site being closer to Nectaris basin than to Imbrium; but the evidence shows that the ejecta produced by the formation of the Imbrium basin reached the floor of Nectaris and beyond, making clear that Nectaris is older than Imbrium and already disproving the first interpretation. The third interpretation is that during an extended period, before the formation of Imbrium, no basins were formed. Using a viscosity model (which estimates the age of the basins based on its isostatic subsidence) and taking into account the Crater Retention Ages (CRAs) and the morphology of the crater rims, the study determined that at least Crisium, Nectaris, Humorum and Werner-Airy were formed prior to Imbrium, with Werner Airy dating back to 4.3 Ga. Baldwin argues that before the formation of these basins a great amount of craters were formed so there was crater saturation, meaning that the CRAs for small craters are not as reliable because of the erasing of them due to ulterior formation of craters. With this analysis, Baldwin separates the formation of these basins enough to a point where they are not being formed in a short enough period of time to justify a Cataclysmic event and refutes the assumptions that support the Terminal Lunar Cataclysm.

Kamata et al. (2015) calculated the thermal evolution and the viscoelastic deformation of multiple basins following the solidification of the Lunar Magma Ocean (LMO). Amongst their results they present that for a viscous relaxation of the topography of the craters that allows the current state of the Prenectaric basins to happen, the lunar Moho temperature must have been higher than 1300 K at the moment of the basins formation. Such temperature can only be maintained for about 50 My after the LMO solidification (which would require a crust of at least 43 km deep), basin degradation of craters allegedly formed in such a window is not consistent with an LHB scenario in which most of these craters were formed around 3.9 Ga as the ages derived from the model places nearly half of the basins formation ages before or around 4.2 Ga.

Analyzing the regolith thickness at several points on the lunar surface, Xie et al. (2021) concluded that lunar impacts decayed monotonically and that their results do not support an LHB.

1.2.4. Hartmann's stone-wall

Hartmann (1975) mentions that amongst the observations that led to the conception of the LHB (back then the Terminal Lunar Cataclysm): "A sharp cut-off in crystallization ages at 4.0 Ga [meaning that] well-preserved older rocks are rare or absent. This has usually been the main observation evoked.", but he argues that it is the consequence of an early heavy bombardment in the lunar history and, therefore, of the formation in a short period of time of what the author calls "mega-regolith" capable of covering most of the prior record without the need for a cataclysmic event (mega-regolith being non-consolidated materials produced in a large scale because of crater formation).

To Hartmann, this early heavy bombardment is due to the high impact rates during the solar system formation and their gradual decrease as the material accreted into planetary embryos and planets. According to this author, this impact flux was enough to produce a number of craters (and ejecta) capable of covering most of the record prior to 4.1 Ga; thus, it is not necessary to consider a cataclysmic event like the LHB. This scenario is referred to as the “stone-wall effect” because “as we probe back in time, we strike a ‘stone wall’ beyond which we cannot get information” (Hartmann, 1975).

Grinspoon (1989) implemented a probability-based model for the age resetting of lunar rocks to assess the generation of lunar age histograms. Using an exponential decline in the crater formation rate on the lunar surface such that “destroying old rocks on the Lunar surface and creating new ones would create a clustering of rock ages at some critical flux level, where the impact rate dropped far enough to let most rocks survive from this time.”, he finds out that it is possible to generate age histograms like those used to propose the LHB hypothesis. In concordance with the stone-wall hypothesis, Grinspoon concludes that a spike in the lunar rock age distribution is a natural consequence of an exponentially declining impact rate. Adding to the fact that there are no other convincing arguments for a Terminal Lunar cataclysm in the literature contemporary to the study.

This model was criticised because of the lack of consideration for the mega-regolith mechanics in the production of dust and clasts present in dated samples that had an important role in the obtention of impact ages (Chapman et al., 2007).

1.2.5. Other arguments

Chapman et al. (2007) examined geochronological evidence both in favour and against an LHB. Concluding that by then, there were no robust enough arguments on both sides of the debate and discusses major biases in the sampling of Moon materials. Regolith dynamics are invoked as a key to understand the impact record of the Moon.

Zellner (2017) made a compilation of new observations about orbital data, lunar meteorites, terrestrial and impact samples ages, and dynamical models. From this information, he concludes that there was not an LHB, but a prolonged bombardment from aprox. 4.2 Ga to 3.5 Ga.

More recently, Hartmann (2019) in an extensive review article where not only the main arguments are revised but also the history of the paradigm. The author discusses the epistemologic problems of the paradigm and how it led to its prolongation. Within many conclusions, the term LHB is suggested to be as initially conceived, and thus making it, not consistent with the observations.

1.3. **Remarks on the LHB**

As shown in the summary presented in Table 1, it is still difficult to state with certainty if the LHB occurred or not. There is a lack of observational evidence to support the dynamic arguments and some deficiencies in the geochemical ones. Most arguments against the occurrence of an LHB (with their respective limitations and discussions) hold up to a point in which the LHB has still to be treated as an open discussion. For the time being, dynamicists seem to have stopped using the LHB as a constraint for the newer models describing the early dynamics of the Solar System but areas like astrobiology and geology seem to still favour the hypothesis as it may complete other hypothesis like those related to the first records of life on Earth (e.g. Von Hegner, 2023).

Table 1. Main arguments for or against the LHB described throughout section 1. It is important to note that the arguments are not shown as arguments paired to their counterargument but rather just as a listing.

In favour	Against
Rock ages showing a concentration around 3.9 Ga and a lack of rocks with older ages (Tera et al., 1974; Cohen, 2000; Cohen et al., 2000).	Open system behaviour on Ar-Ar ages of lunar samples (Boehnke & Harrison, 2016; Harrison et al., 2018) and early ideas suggesting age saturation (Hartung, 1974; Wetherill, 1975).
Nice-like models suggest that late instabilities could have enabled a LHB (e. g. Gomes et al., 2005; Morbidelli et al., 2012).	Current dynamical models favour an early instability scenario (e.g. Clement et al. 2023, Nesvorny et al. 2023, Izidoro et al. 2024).
Proposal of 2 periods of intense bombardment on Earth from impact spherulites (Lowe & Byerly, 2018).	Stone-wall hypothesis (Hartmann, 1975).
Finding of LHB-like behaviours on other stellar systems (Lisse et al., 2012, 2016)	Dating of planetary materials showing no evidence of a LHB (e.g. Walton et al. 2023, White et al. 2024).
Tracing of the last ancestor of bacteria being consistent with the LHB temporality (Fournier et al., 2022).	Age estimation of basins based on their isostatic subsidence and stratigraphic analysis (Baldwin, 2006).
Inference of a LHB and an Early Heavy Bombardment from LOLA data (Frey et al., 2016).	Discrepancy between thermal evolution of the LMO and observed viscous relaxation of multiple basins related to the LHB (Kamata et al., 2015).

2. Methodology

The goal of this study is to model the stone-wall effect to contribute to the discussion on the LHB and the dynamics of the early solar system. To do so it is necessary to: a) estimate the number of impacts occurred on the surface of the Moon from 4.1 to 3.8 Ga, as well as the size distribution of the impact craters formed (sections 2.1 and 2.2), b) generate randomly a set of coordinates to simulate the places of crater formation (section 2.3), and c) determine the percentage of the Moon surface area covered by the craters and their continuous ejecta considering not the sum of individual crater areas but the calculation of the total area of the overlapping craters (section 2.4). Figure 1 shows the details of the methodology which will be set forth through the following sections.

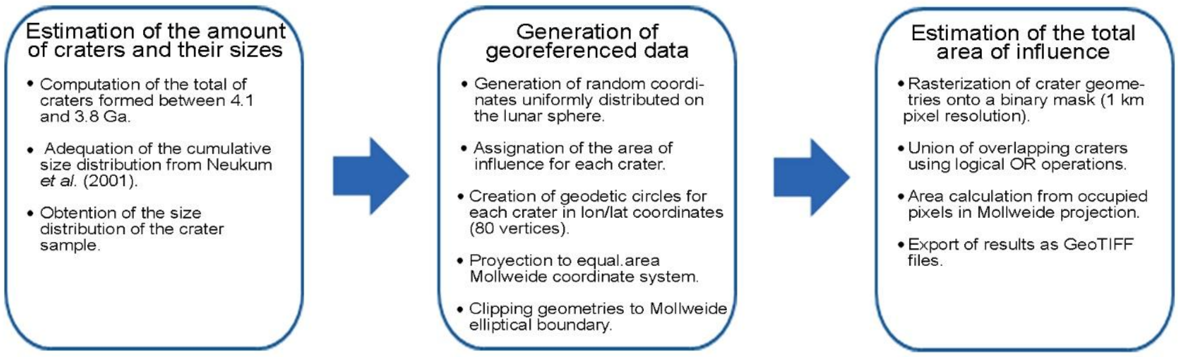

Figure 1. Workflow employed.

2.1. Number of craters formed between 4.1 and 3.8 Ga

To model the stone-wall hypothesis, first it is necessary to estimate the total number of impact craters formed on the Moon's surface between 4.1 and 3.8 Ga. Here, it is important to make clear a point: in the Introduction, we mentioned that the LHB period is between 4.2 and 3.8 Ga, but we did calculations from 4.1 Ga to 3.8 Ga because one of the equations that we used (eq. 1), is not valid for ages greater than 4.1 Ga (Schmedemann et al., 2014), then our results represent a lower limit. The function employed was proposed by Neukum et al. (2001) which relates the number of craters per square kilometre, N, with a diameter D equal or greater to 1 km with the crater accumulation time T in Ga. According to these authors, it is expressed as shown:

$$N(D \geq 1\ km, T) = 5.44 \times 10^{-14}\ (e^{6.93T}\ - 1) + (8.38 \times 10^{-4})\ T. \quad (1)$$

Subtracting the result of equation (1) for T = 3.8 Ga from the result for T = 4.1 Ga and multiplying by the surface area of the Moon (37,932,328.1 km^2), we obtained the total number of impact craters with diameters greater or equal than 1 km formed between 4.1 and 3.8 Ga:

$$N_{tot} = 37{,}932{,}328.1\ km^2\ \times N(D \geq 1km, 4.1 \geq\ T \geq 3.8) = \qquad (2)$$

$$3.8 \times 10^7 km^2 \times [N(D \geq 1km, 4.1)\ -\ N(D \geq 1km, 3.8)].$$

Thus, yielding 3,955,909 craters formed on the lunar surface during the LHB temporality. Note the rounding of the result as there is no such thing as crater fractions.

2.2. Size distribution of the craters

To derive the size distribution for the craters formed between 4.1 and 3.8 Ga, we used the 11th degree polynomial proposed by Neukum et al. (2001) to describe the number of craters with a diameter greater than D formed per square kilometre for a period of 1 Gyr. This function has the property of preserving its general form at any given time:

$$log_{10}[N(> D)] = \sum_{j=0}^{11} a_j \times\ \ [log_{10}(D)\ ]^j \qquad (3)$$

where D is the diameter in kilometers and a_j are coefficients with a time dependency. This function is valid for craters from 100 m to 200 km in diameter, thus in this work, we only considered those with a diameter greater than 1 km and less than 200 km to maintain concordance between the domains of equations (1) and (3).

To assess the size distribution function for the LHB temporalities, the function was discretized by generating intervals in a similar way to the HPF (Hartmann Production Function) (Neukum et al., 2001) so that:

$$D_{up} = D_{lo}\sqrt{2}, \qquad (4)$$

where D_{lo} is the lower limit and D_{up} the upper limit of each interval. The minimum value for D_{lo} is 1 km and the highest value for D_{up} must be lower than 200 km. The midpoint of each interval is calculated and used in equation (4) to assign this value to the whole interval. This gives a discrete function for a 1 Gyr period. To adjust the function in time for 4.1 to 3.8 Ga, it is necessary to normalise the data. To do this, the calculated value of each interval must be divided by that of the first bin (16,925 craters). The normalised values obtained are multiplied by the total number of craters formed during the LHB temporality (3,955,909 craters). The result is a cumulative discrete function for the sizes of the craters formed from 4.1 to 3.8 Ga (Fig. 2).

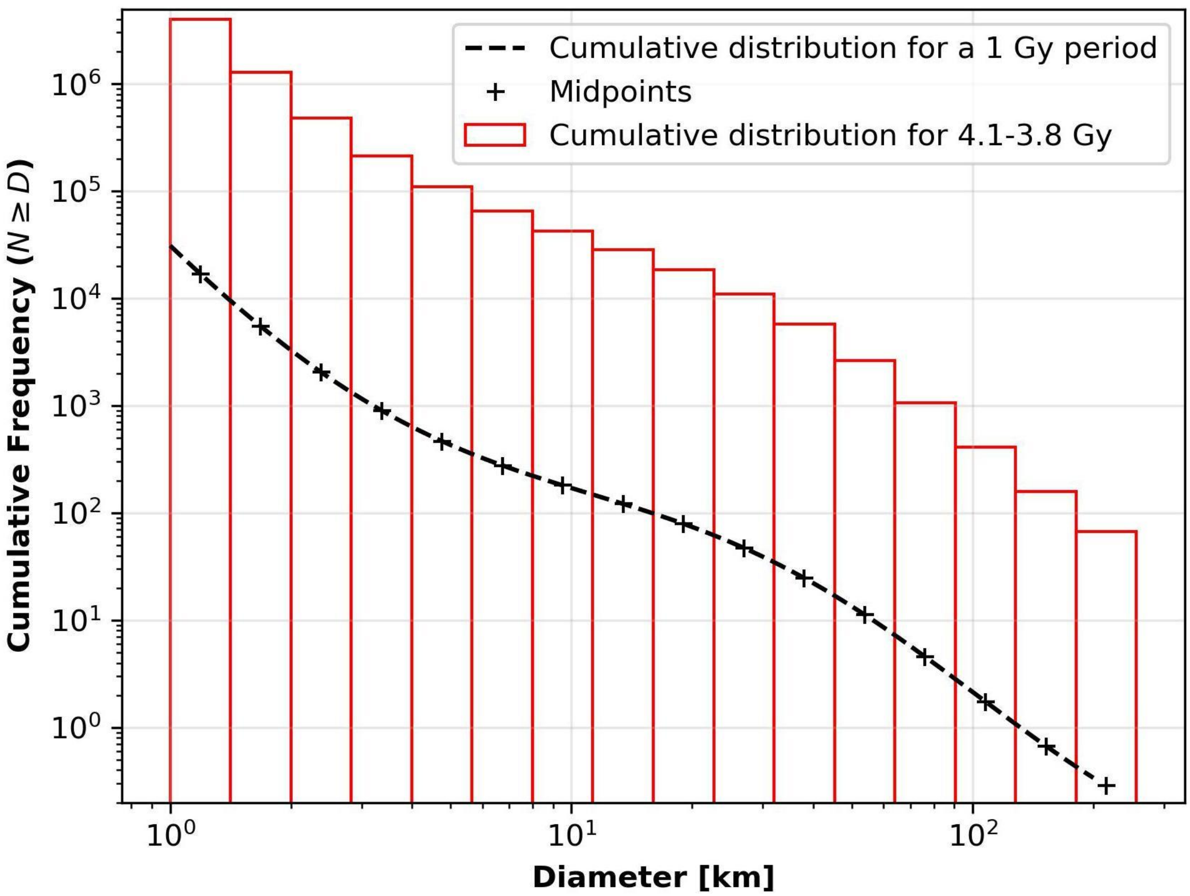

Figure 2. Cumulative crater distribution adequate to the LHB temporality as described in Section 2.2.

To obtain the number of impact craters in each size interval, formed between 4.1 and 3.8 Ga, we subtracted to each value in the cumulative distribution in Figure 2, the value of the next interval. Resulting in the distribution shown in Figure 3. Note that the total number of craters shown in Figure 3 is 3,955,842 which is less than 3,955,909 because there are 67 craters with diameters greater than 181 km, and we did not consider greater craters because the next interval (181, 256) contains craters with diameters that are outside the domain of equation (3).

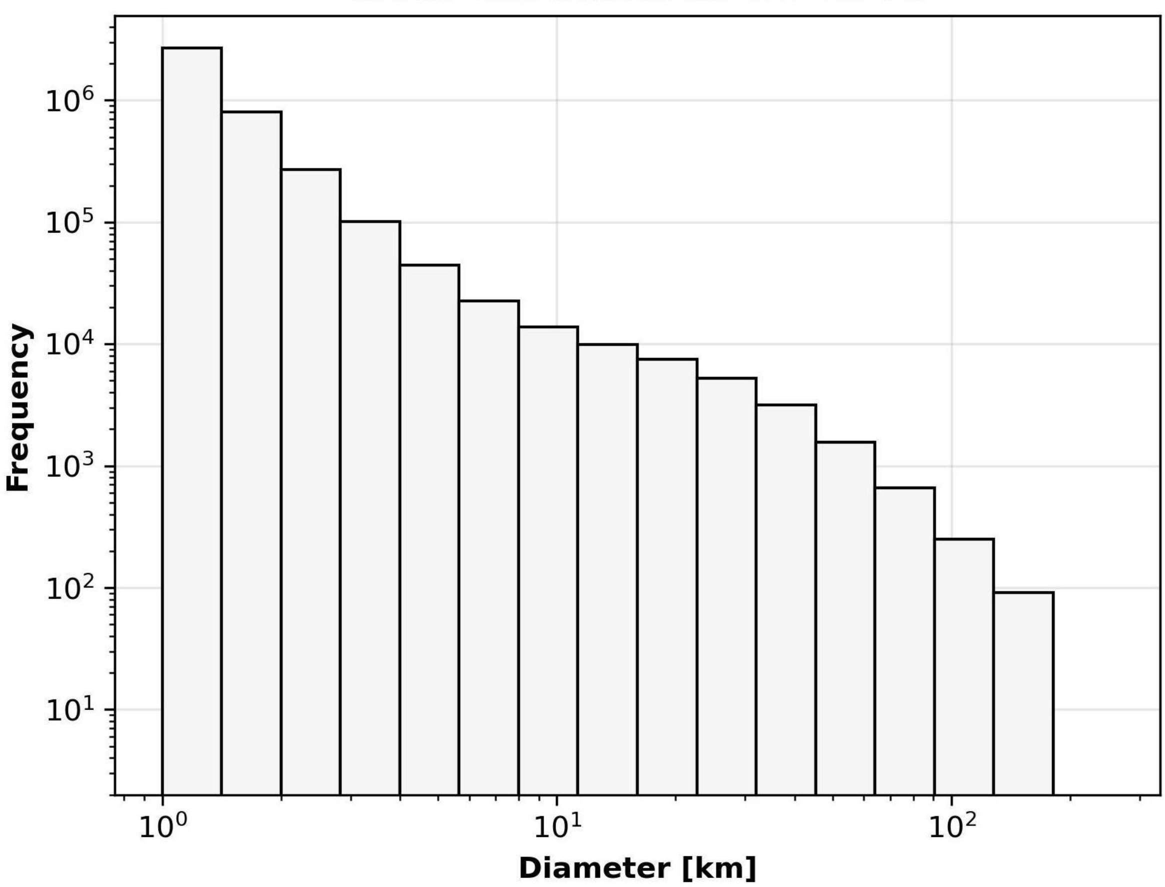

Figure 3. Final crater size distribution employed. Each bar shows the number of impact craters with sizes between Dlo and Dup, formed between 4.1 Ga and 3.8 Ga.

Stöffler and Ryder (2001) reevaluate the impact lunar flux by means of a detailed study of lunar stratigraphy, and relative and absolute age dating. To assess our proposal for the cumulative crater distribution adequate to the LHB temporality, we digitized some curves from the figure 5 in the cited paper and compared them with the data represented by red bars on figure 2. To do so, it was necessary to multiply the digitized data times the lunar area (figure 4). The blue curve represents the cumulative number of craters obtained as described a few paragraphs above. According to Stöffler and Ryder (2001), the pre-Nectarian period span between the Moon formation and 3.92 Ga approximately, then the orange curve shows the cumulative impact craters that characterizes lands of this age. The blue curve shows a greater number of impact craters smaller than 50 km and less craters above said size than the orange curve. However, they are similar, then we can say that our cumulative size distribution function is a reasonable approach to the impact craters formed between 4.1 Ga and 3.8 Ga.

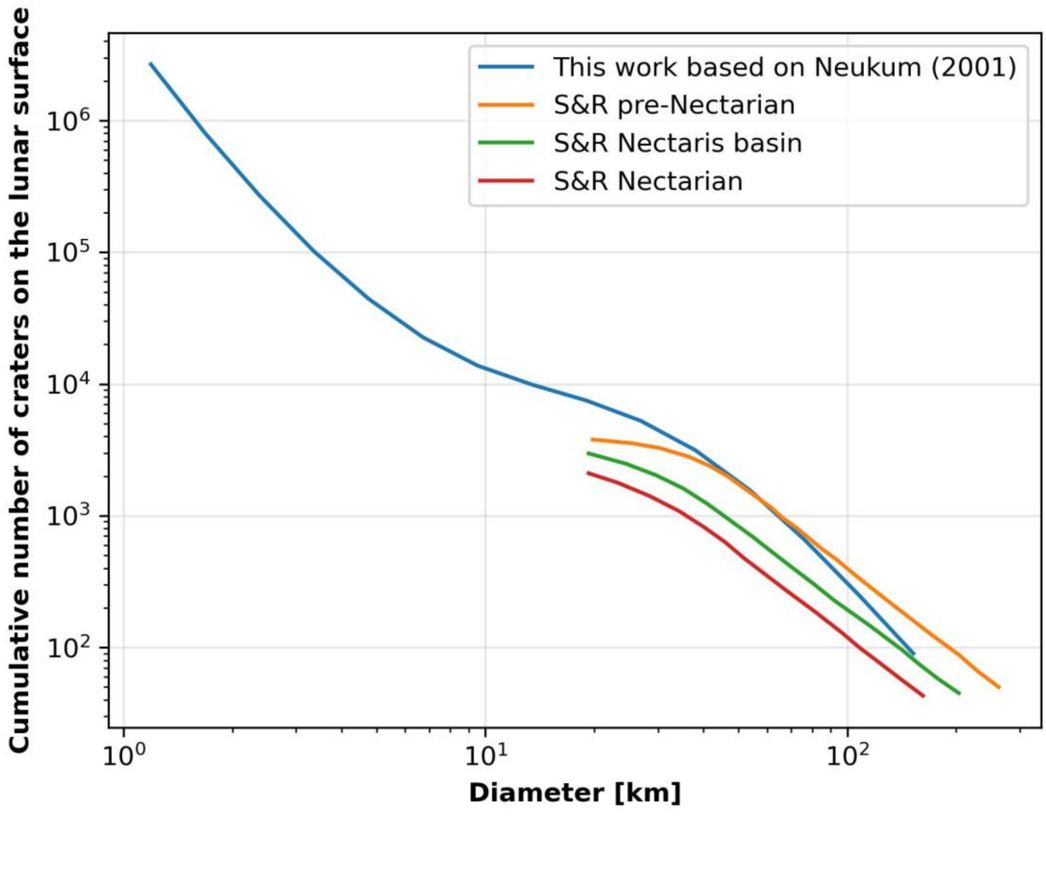

Figure 4. Comparison between the cumulative number of craters formed between 4.1 and 3.8 Ga (figure 2) and the data derived from the figure 5 in Stöffler and Ryder (2001) (S&R in this plot).

2.3. Scattering the craters on the moon's surface

Crater positions were distributed uniformly over the lunar sphere using spherical coordinate sampling. To avoid polar clustering that would result from direct uniform sampling in latitude and longitude, a corrected sampling method was employed: latitude was derived from a uniform distribution of sin(lat) in the interval [-1, 1], while longitude was sampled uniformly in the range [0°, 360°]. This transformation ensures an equal-area distribution of crater centers across the entire lunar surface, consistent with the assumption of spatially homogeneous bombardment.

2.4. Buffer area of the craters

The buffer area or area of influence of an impact is given by the crater and its continuous ejecta. For simplicity, we assumed that the craters are circular, and their continuous ejecta is emplaced radially and uniformly in a similar shape. An approximation made by Melosh (1989) suggests that the extension of the continuous ejecta blanket is about 1 crater radius, but to assess the sensitivity of our results to the ejecta extent assumption, we performed additional analyses with alternative ejecta extension of 0.5 Rc and 1.5 Rc, then the buffer area of each crater as circles whose radius, R_{buf}, is given by:

$$\mathrm{R}_{buf} = \mathrm{Rc} + \varepsilon \, \mathrm{Rc} \tag{5}$$

where Rc is the crater radius; and the product, ε Rc, represents the ejecta's extension so that in the sensitivity test we used ε values of 0.5, 1.0 and 1.5. The main results presented in this study correspond to ε = 1.

Since the formation of craters on the Moon is considered to be random, to assess the coverage consistency throughout different uniform spatial distributions, ten different sets of 3,955,842 randomly generated coordinates on the lunar sphere were created. To each of these points, a radius Rc was assigned according to the size distribution function calculated in section 2.2 and R_buf was calculated for each according to equation (5). These ten sets were only done for ε = 1.

Additionally, to analyze the temporal evolution of crater coverage, the bombardment period from 4.1 to 3.8 Ga was divided into successive intervals of 0.01 Ga (10 million years). For each interval (4.1 Ga, T), crater populations were generated, representing all impacts that occurred between time T and the reference time 4.1 Ga. This incremental approach allowed tracking how the lunar surface coverage evolved throughout the Late Heavy Bombardment temporalities, with 30 time steps covering the entire period. This complete temporal analysis was performed independently for each of the three buffer radius scenarios described above (ε = 0.5, 1.0, and 1.5).

To estimate the area covered by lunar craters and their ejectas, a geospatial methodology was developed based on geodesic geometry on a spherical model of the Moon (Figure 1, middle and right boxes). Since the Moon can be approximated as a perfect sphere, a selenographic coordinate reference system (CRS) with a constant radius of 1,737.4 km was defined. This system allowed working directly on angular coordinates adapted to the lunar geometry. Based on this CRS, polygonal representations of each crater were generated by constructing geodetic circles centered on the coordinates of each crater and their respective radius. These circles were approximated by sampling 80 equiangular points along the geodesic boundary.

A systematic accuracy analysis was performed using the largest basin from the 26 major impacts considered in this study (Imbrium basin, D = 1,160 km) (Table 2), demonstrating that 80 vertices yield a relative error of only 0.12% compared to the theoretical spherical cap area (equation 6), while configurations with fewer vertices (e.g., 10-40) produced errors exceeding 0.5 - 7%.

$$Area = 2\pi {R_M}^2 \left(1 - \cos\left(\frac{R_{buf}}{R_M}\right)\right), \tag{6}$$

where R_M is the radius of the Moon (1737.4 km).

Special attention was given to craters crossing the antimeridian (±180° longitude), which were automatically split into two separate polygons to avoid topological errors during projection.

The generated geometries were reprojected to an equal-area Mollweide projection centered on the Moon. This reprojection is essential to ensure that the area calculations are faithful to the actual proportions on the spherical surface of the Moon.

Area calculation was performed through rasterization to handle the massive number of overlapping craters efficiently. Each crater polygon was rasterized onto a binary mask with a 1 km pixel resolution using the center-point method, where a pixel is considered covered (value = 1) only if its center falls within the crater polygon boundary. Precision testing across multiple pixel resolutions (100 m to 5 km) using the Imbrium basin showed that pixel sizes between 100 m and 2 km produce nearly identical relative errors (< 0.13%). The 1 km resolution was selected as it offers the optimal trade-off between accuracy (< 0.12% error) and computational performance (processing time reduced by 50% compared to 100 m resolution), while coarser resolutions (5 km) may underestimate small crater contributions.

Individual masks were combined using logical OR operations, ensuring that pixels covered by any crater are marked. The final union area was computed by counting occupied pixels and multiplying by the pixel area (1 km²). This raster-based approach allows accurate estimation of total covered area while accounting for overlapping craters, avoiding the memory limitations of vector-based spatial dissolution.

3. Results

From the 10 runs, the resulting average percentage of the Moon's surface area covered by the craters and their continuous ejecta was equal to 95.7%, with a standard deviation of 0.08 % (from the average percentage). This last data indicates that the ten runs give very similar results.

To explain this consistency, an estimation of the area affected by the total of craters formed between 4.1 and 3.8 Ga without considering overlapping was made. For each diameter associated with each bin, the area of influence was calculated using the area of a circle on the surface of a sphere whose radius is that of the Moon. In this case the area of the circles is given by equation (6).

Figure 5 shows the normalised cumulative distribution function for the areas covered by the craters employed. Here it is observed that 51.6% of the affected area is due to craters greater than 38 km (5, 696 craters) which represents 0.14% of the total craters. This means that the area covered by craters greater than 38 km is meaningfully greater than that covered by craters with a lower diameter. On the other hand, the total buffer area of the crater population was calculated without considering the overlapping giving as a result a coverage area of 119,798,529.5 km^2 which is close to thrice that of the Moon's surface. Thus, this shows that our model is more representative of the "stone-wall" effect than the sole sum of the areas.

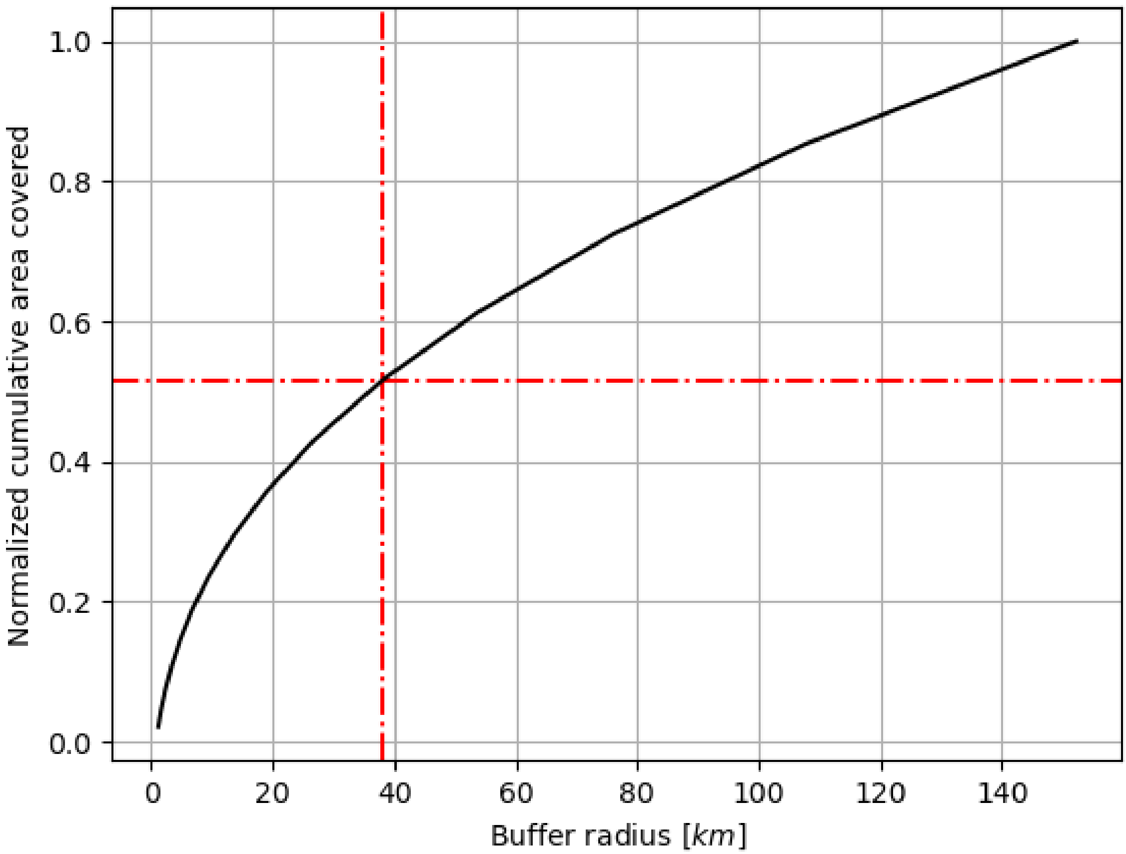

Figure 5. Comparison of the cumulative area of circles on a sphere with the Moon's radius for ε =1. The vertical red line corresponds to a Rbuff of 38 km, and the horizontal red line indicates a normalized cumulative area of ~50 %.

Figure 6 shows the number of craters with diameter D equal or greater to 1 km and less than 200 km formed on the lunar surface from 4.1 Ga to 3.8 Ga according to equation (1). These values were used to assess the area covered by the impact craters for each of the 30 time steps mentioned in section 2.4.

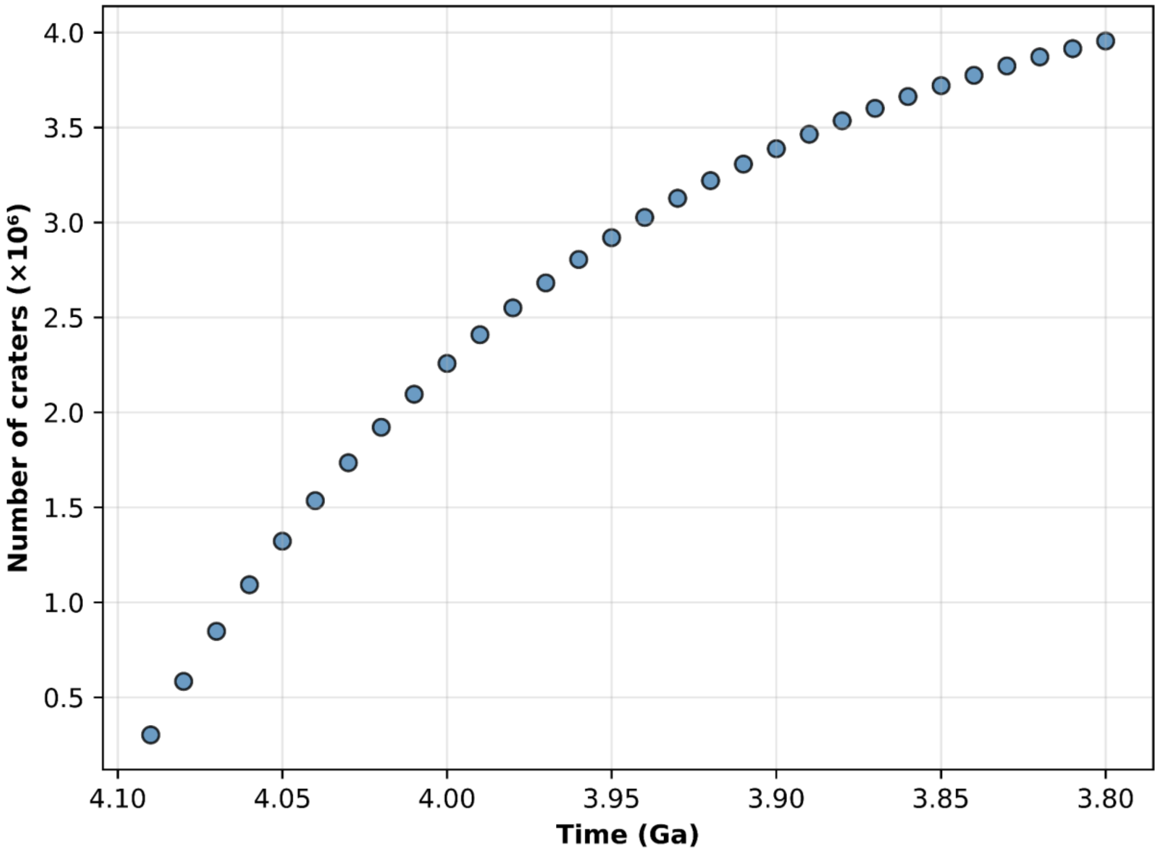

Figure 6. Number of impact craters formed on the lunar surface from 4.1 Ga to 3.8 Ga.

The temporal evolution analysis described in section 2.4 allowed us to better observe the change in the coverage and overlapping efficiency. In the nominal case of this study ($\mathcal{E}$ = 1), represented in figure 7, it is possible to observe a converging behaviour towards near the surface area of the Moon as shown in figure 8. Whilst the overlapping efficiency tends to drop as the surface reaches saturation (Figure 9). Note that in this study the overlapping efficiency is the comparison between the total area of the craters and the total area covered when taking into account the effect of the overlapping.

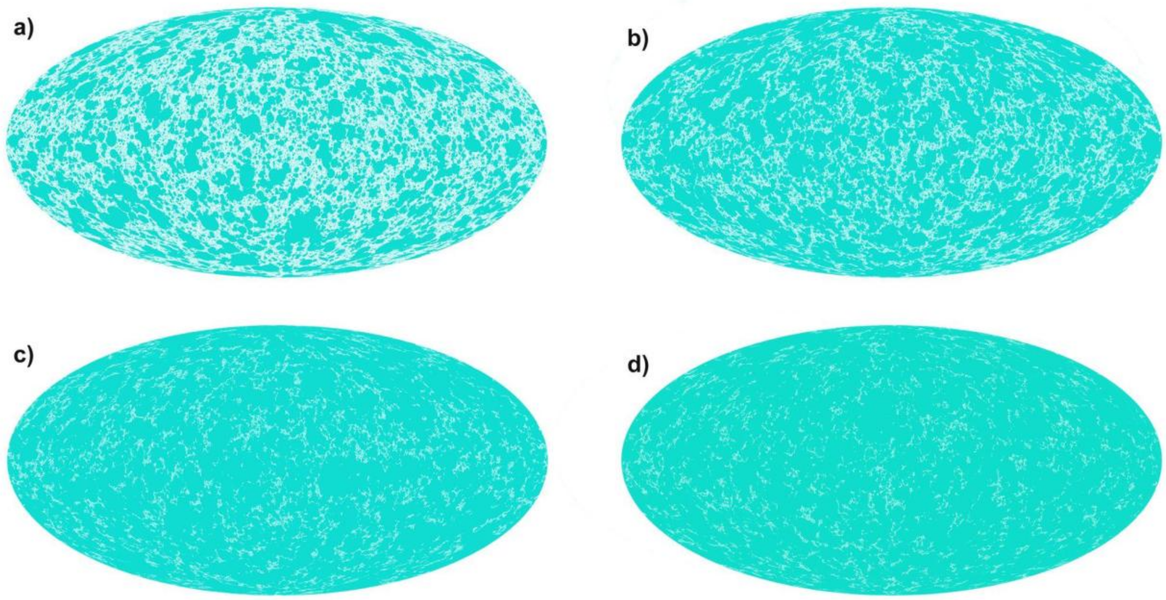

Figure 7. Evolution of formation of impact craters on the Moon. This figure shows only four stages from the 30 time steps described in section 2.4, when $\mathcal{E}$ = 1. Impact craters formed between 4.1 Ga and: a) 4.05 Ga, b) 4.0 Ga, c) 3.9 Ga, and d) 3.8 Ga.

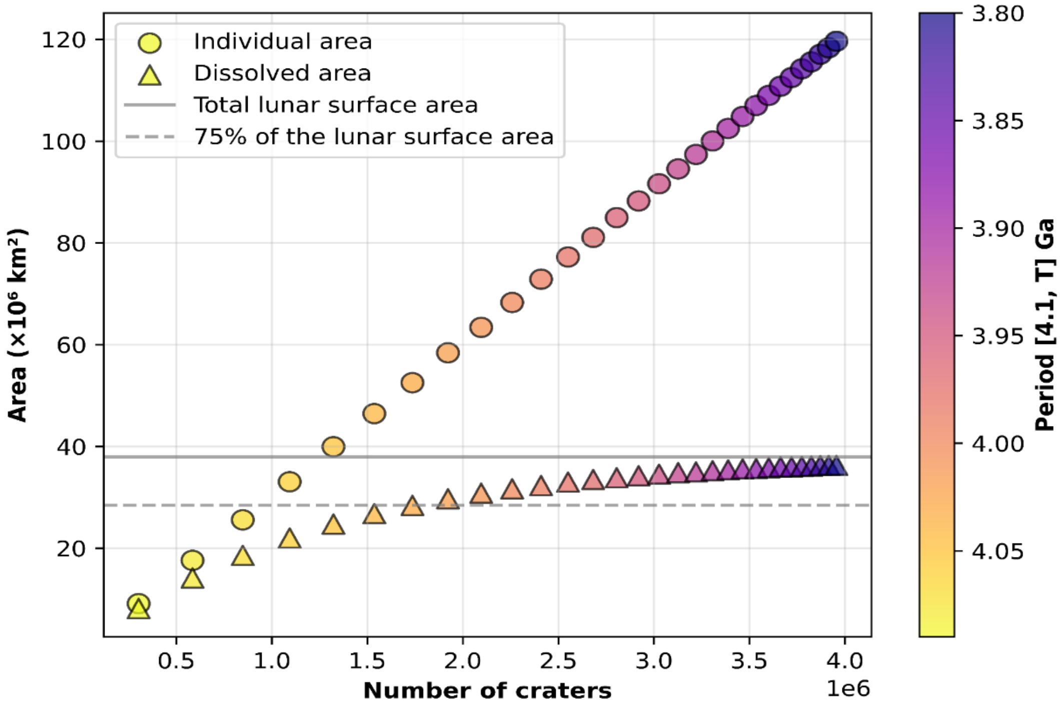

Figure 8. Area covered by impact craters and their continuous ejecta with and without considering their overlapping. Circles show the values of the area covered without considering overlapping while triangles show the results with overlapping. The color

bar represents the value of T where it is the upper limit of the interval of time in which the impact craters were formed.

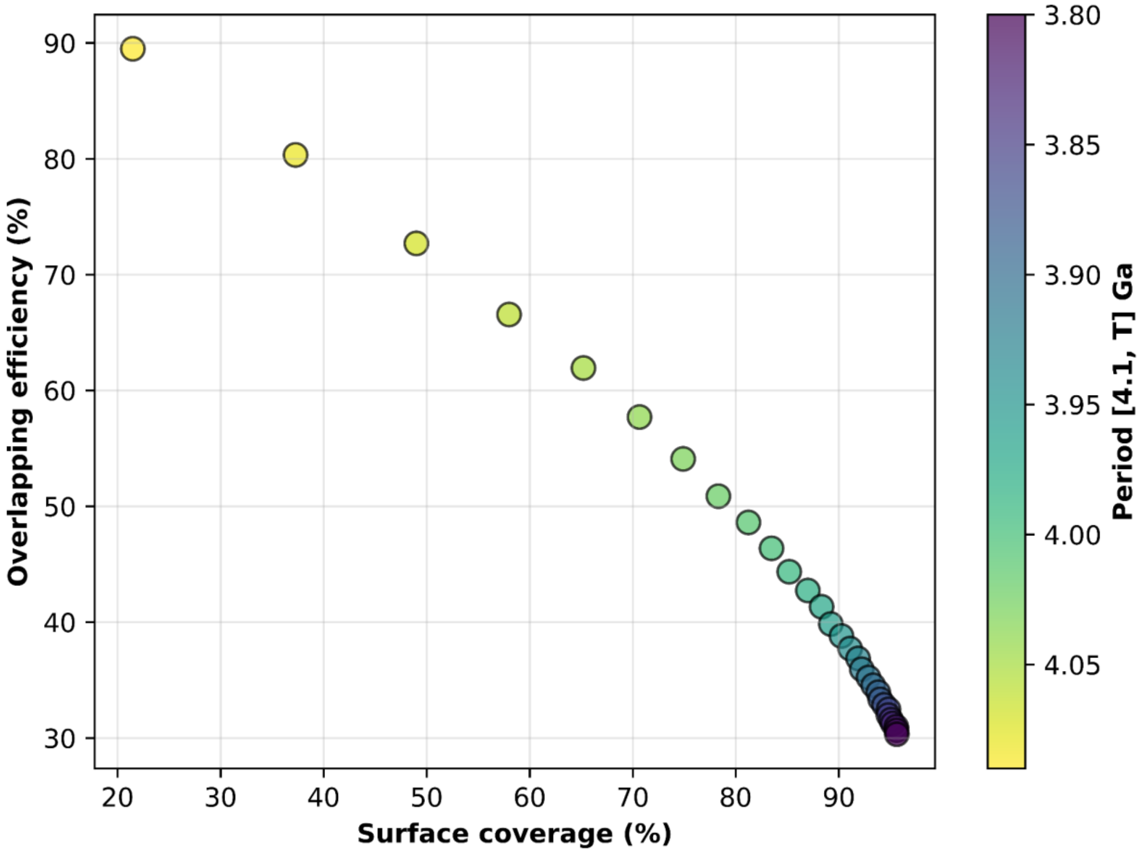

Figure 9. Overlapping efficiency vs surface coverage for $\mathcal{E}$ = 1. Read the text for more details. The bar at the right has the same meaning of the bar in the figure 8.

For the cases where $\mathcal{E}$ = 0.5 and 1.5, represented in figures 10 and 11, the rate at which the surface gets covered is then affected as shown in figure 12. At $\mathcal{E}$ = 1.5, full coverage of the surface area of the Moon is almost reached within the LHB temporalities. For lower $\mathcal{E}$ values, full coverage is not reached but similar behaviours are expected as time increases under the same bombardment regime. Comparing the results for the full period (4.1 Ga - 3.8 Ga), the covered area was 83 % for $\mathcal{E}$ = 0.5, 95.7 % for $\mathcal{E}$ = 1.0 and 99.2 % for $\mathcal{E}$ = 1.5.

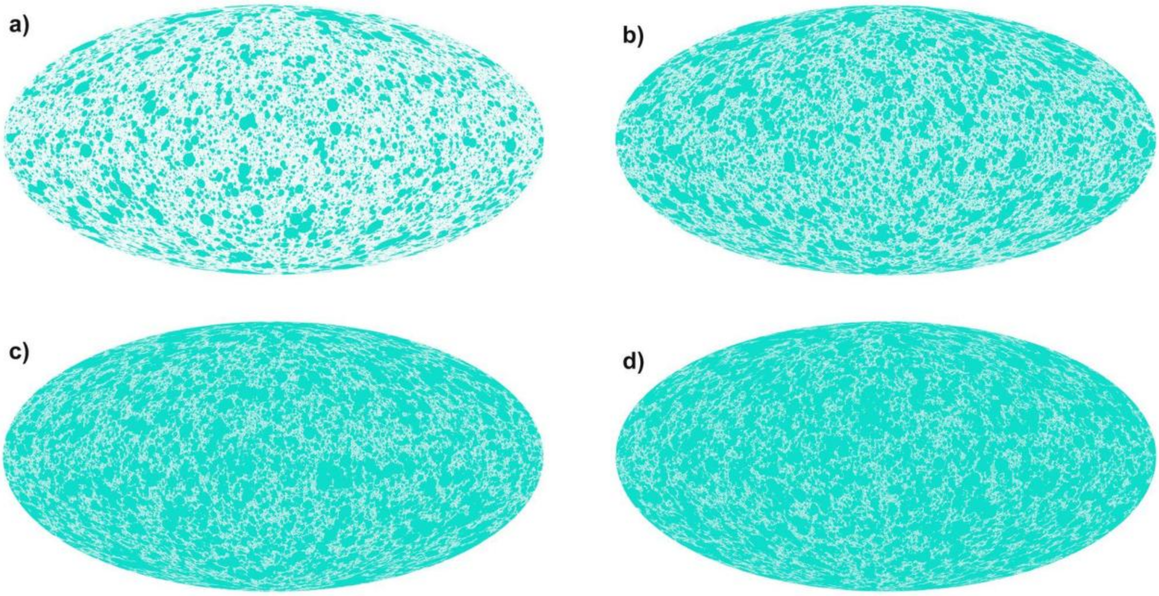

Figure 10. Evolution of formation of impact craters on the Moon. This figure shows only four stages from the 30 time steps described in section 2.4, when $\mathcal{E}$ = 0.5. Impact craters formed between 4.1 Ga and: a) 4.05 Ga, b) 4.0 Ga, c) 3.9 Ga, and d) 3.8 Ga.

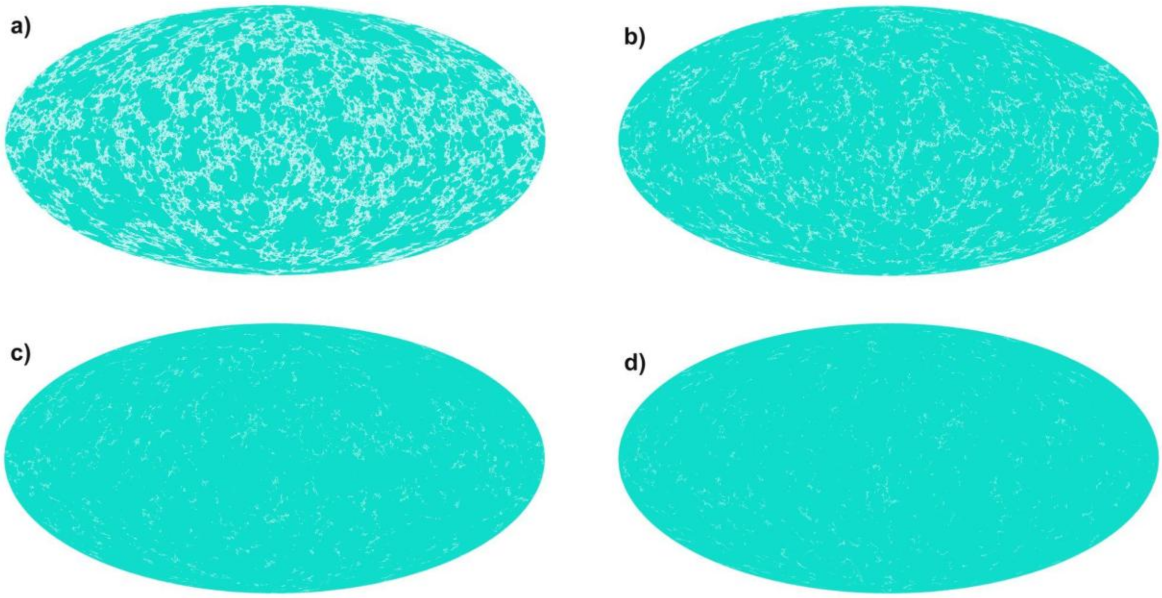

Figure 11. Evolution of formation of impact craters on the Moon. This figure shows only four stages from the 30 time steps described in section 2.4, when $\mathcal{E}$ = 1.5. Impact craters formed between 4.1 Ga and: a) 4.05 Ga, b) 4.0 Ga, c) 3.9 Ga, and d) 3.8 Ga.

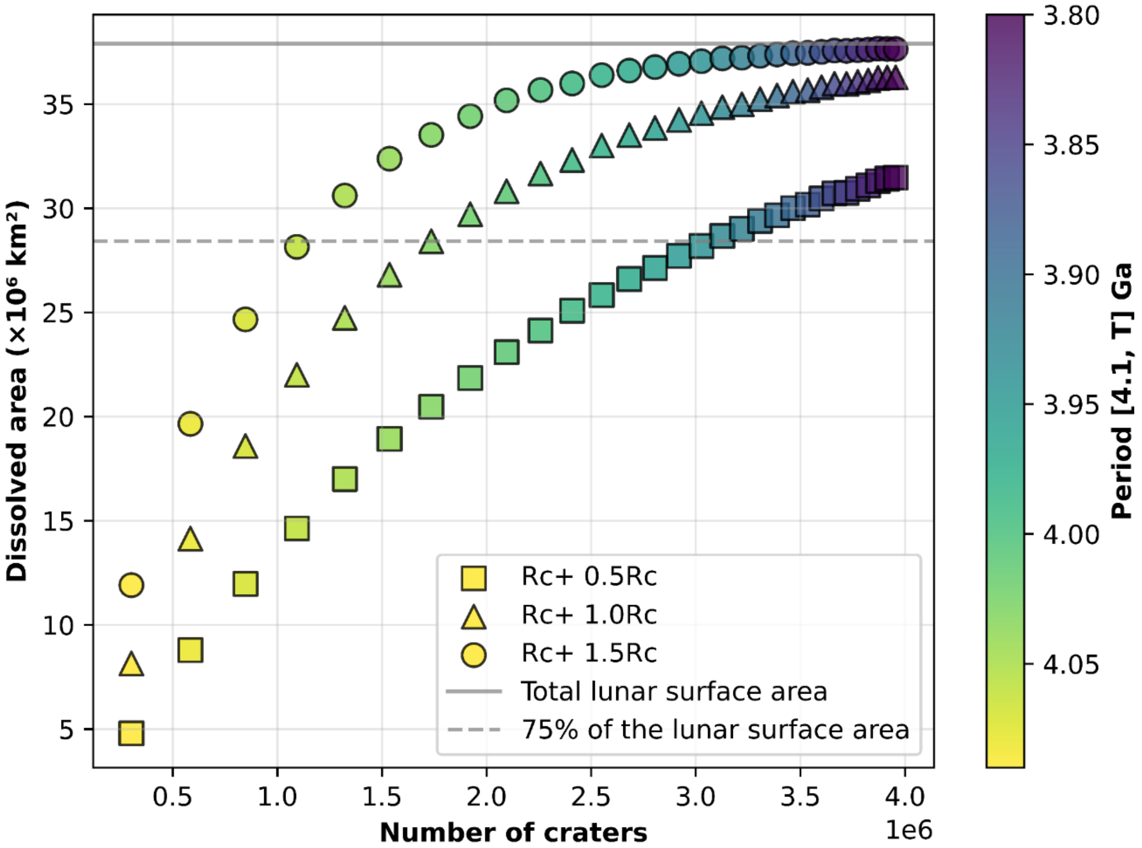

Figure 12. Area covered by impact craters and their continuous ejectas considering three possible ejecta's extension: 0.5 Rc, 1.0 Rc, and 1.5 Rc. The bar at the right has the same meaning of the bar in the figure 8.

On the other hand, we estimated the area affected by the 26 major basins formed between 4.2 Ga and 3.8 Ga (Table 2). Basins of these sizes were not considered in our model because they are out of the domain of equations (1) and (3) . When we made a new run considering only these 26 basins in their current locations, the coverage is ~50 % of the surface area of the Moon (Fig. 13). This further highlights the fact that larger craters are the main factor behind the resurfacing of the Moon.

Table 2. Twenty-six basins formed between 4.2 and 3.8 Gy.

Basin[a]	Diameter [km]
Coulomb-Sarton[g]	530
Dirichlet-Jackson[c]	470
Cruger-Sirsalis[f]	475
Smythii[g]	840
Schiller-Zucchius[g]	325
Amundsen-Ganswindt[d]	335
Nubium[g]	690
Poincaré[b]	319
Lorentz[e]	312
Birkhoff[e]	345
Ingenii[h]	282
Serenitatis[g]	740
Apollo[e]	537
Nectaris[g]	860
Korolev[e]	437
Mendeleev[e]	313
Hertzprung[e]	591
Grimaldi[g]	430
Planck[e]	314
Moscoviense[h]	275.57
Crisium[g]	1060
Humorum[g]	825
Humboldtanium[h]	230.78
Imbrium[g]	1160
Schrödinger[e]	312
Orientale[g]	930

[a]Basins ordered stratigraphically (oldest to newest) according to Fassett et al. (2012).
Basin diameters according to: [b]Andersson & Whitaker (1982); [c]Cook et al. (2000); [d]Hady et al. (2016); [e]McDowell (2007); [f]Singh et al. (2022); [g]Wilhelms et al. (1987); [h]USGS (n.d.).

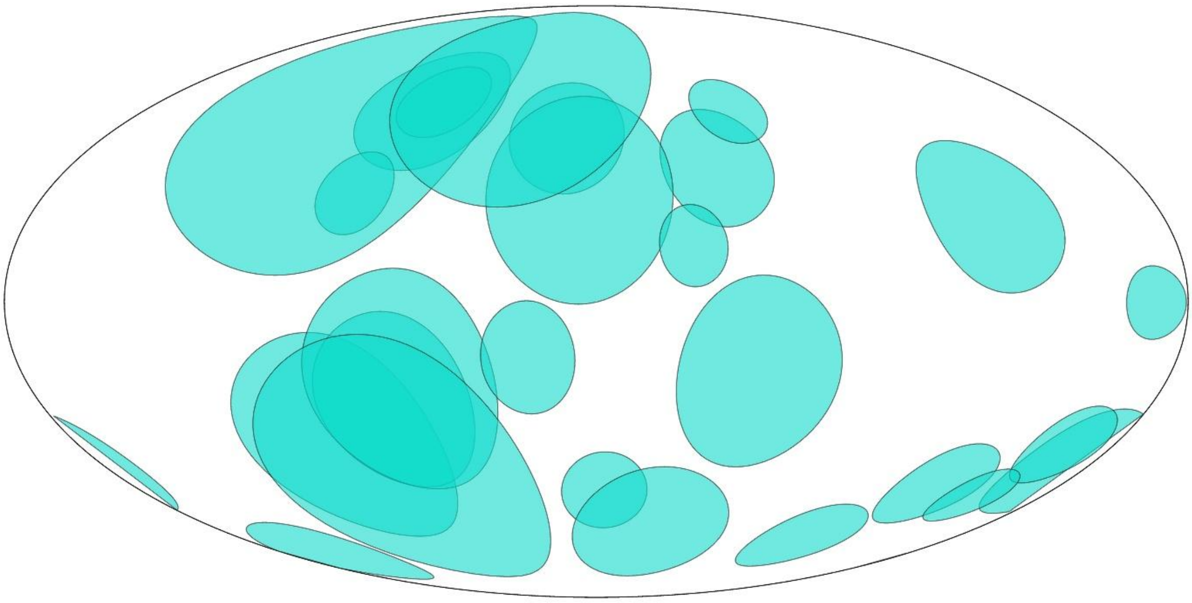

Figure 13. Resulting map of the 26 basins formed between 4.2 and 3.8 Ga.

4. Discussion

It was observed that the craters with a diameter equal to or greater than 38 km had the most influence over the area covered, even though the number of smaller craters is much greater. Using craters with a diameter equal to or greater than 1 km, due to the validity of the equations employed, could be a limitation of our model because smaller craters could increase the area covered even in a barely significant scale, supporting our results as a lower limit. Additionally, it was found that the 26 basins formed during the alleged LHB temporality affected ~50 % of the surface area of the Moon.

Given that the erosive factors of the impact record of the Moon is mainly driven by large impacts, most of this record is said to be well preserved all the way to ~4 Ga. Other factors such as space weathering and small impact erosion whilst being important at certain scales, when looking at a global picture of the problem such sources become negligible.

Another factor that can be brought up can be the uniform distribution of the craters on the Moon's surface used in our model. Gravitational asymmetries are not thought to be mentioned in the literature as factors shaping the distribution. Although, tidal locking does seem to produce an "apex-antapex" effect where the leading hemisphere presents up to 2.68 times more craters of diameters 1-20 km (Zhao et al., 2024). This effect seems to affect smaller craters, but no information is given for larger craters. Due to the behaviour of larger craters on the surface coverage discussed already, such an effect is not likely to affect the results.

Regarding the approximation employed for the radius of the buffer area, even though it is a valid one since it is based on observations (Melosh, 1989), assuming the same factor for all crater sizes can be regarded as simplistic and future models should aim to better approximate said radius. This could be done by obtaining data from ballistic experiments and simulations for the different crater size ranges and shapes to constrain in more detail the behaviour of ejecta and thus, the behaviour of the area covered by it.

Another area of discussion is the relationship between the results obtained in this study, concerning the LHB, the Nice Model, and the Grand Tack model. The Grand Tack model was proposed as a solution to the "small Mars" problem, whilst the Nice model was proposed as a mechanism to allow the occurrence of an LHB. Both models have evolved in such a way that the final conditions of the first model are similar to the initial conditions of the Nice model, making both models mutually compatible and thus candidates as solutions for their respective problems (the small Mars and LHB). The results of this study and the lack of observational evidence for both models mentioned, opens up the possibility for new explanations for the small Mars problem, because our results show that it is very possible that an LHB have not occurred, so the small Mars problem solution not necessarily has to be considered as a constraint and would have to be consistent with current early instability scenarios rather than late instability ones as discussed in Section 1.2, 1.3 and Table 1.

5. Conclusion

Even on a simple scenario in which the buffer area is comprised only by the crater itself and its continuous ejecta, the model showed that without considering a rise on the impact frequency as the one proposed by the LHB hypothesis, the formation of craters between 4.1 and 3.8 Ga was able to affect most (83.0-99.2%) of the lunar surface and thus its geologic record, lowering the odds of sampling rocks with ages older than 4.1 Ga. An additional consideration is that the impact flux from 3.8 Ga to the present day must have further affected the lunar surface.

This result and the lack of observational dynamic evidence in the solar system to support an LHB, implies that a scenario like the one proposed by the Nice model is not necessary to explain the Moon’s impact record and the final conditions of the Grand Tack model are no longer attached to it, leaving room for new proposals to explain the small Mars problem.

Acknowledgements

This work was supported by the Universidad Nacional de México in the form of the “Becas de Titulación - Egresados extemporáneos 2022-2023” grant.

References

Andersson, L. E., & Whitaker, A. (1982). NASA Catalogue of Lunar Nomenclature. *NASA Reference Publication*, *1097*.

Baldwin, R. B. (2006). Was there ever a Terminal Lunar Cataclysm?. With lunar viscosity arguments. *Icarus*, *184*(2), 308–318. https://doi.org/10.1016/j.icarus.2006.05.004.

Boehnke, P., & Harrison, T. M. (2016). Apparent Late Heavy Bombardments. *79th Annual Meeting of the Meteoritical Society*, *22*.

Cartwright, J.A., Hodges, K.V. and Wadhwa, M. (2022). Evidence against a Late heavy bombardment event on Vesta. *Earth and Planetary Science Letters*, 590. https://doi.org/10.1016/j.epsl.2022.117576.

Chapman, C. R., Cohen, B. A., & Grinspoon, D. H. (2007). What are the real constraints on the existence and magnitude of the late heavy bombardment? *Icarus*, *189*(1), 233–245. https://doi.org/10.1016/j.icarus.2006.12.020.

Clement, M. S., Chambers, J. E., Kaib, N. A., Raymond, S. N., & Jackson, A. P. (2023). Mercury's formation within the early instability scenario. *Icarus*, *394*, 1–24. https://doi.org/10.1016/j.icarus.2023.115445.

Cohen, B. A. (2000). *Geochemistry and 40Ar-39 Ar geochronology of lunar meteorite impact melt clasts*. University of Arizona.

Cohen, B. A., Swindle, T. D., & Kring, D. A. (2000). Support for the Lunar Cataclysm Hypothesis from Lunar Meteorite Impact Melt Ages. *Science*, *290*(5497), 1754–1756. https://doi.org/10.1126/science.290.5497.1754.

Cook, A. C., Watters, T. R., Robinson, M. S., Spudis, P. D., & Bussey, D. B. J. (2000). Lunar polar topography derived from Clementine stereo images. *Journal of Geophysical Research: Planets*, *105*(E5), 12023–12033. https://doi.org/10.1029/1999JE001083.

Day, J. M. D., & Neal, C. R. (2024). Evidence for Late Heavy Bombardment "Cataclysm" to the Moon from impact ejecta. *Lunar and Planetary Science* 55.

Fassett, C. I., Head, J. W., Kadish, S. J., Mazarico, E., Neumann, G. A., Smith, D. E., & Zuber, M. T. (2012). Lunar impact basins: Stratigraphy, sequence and ages from superposed impact crater populations measured from Lunar Orbiter Laser Altimeter (LOLA) data. *Journal of Geophysical Research: Planets*, *117*(2), 1–13. https://doi.org/10.1029/2011JE003951.

Fournier, G., Rangel, L. T., Moore, K., Payette, J., Momper, L., and Bosak, T. (2022). Molecular Clock Dates for Bacterial Origins are consistent with Impact Bottleneck Scenarios, EGU General Assembly 2022, Vienna, Austria, 23–27 May 2022, EGU22-8987, https://doi.org/10.5194/egusphere-egu22-8987.

Frey, H. V. (2016). Comparing the early and late heavy bombardments on the Moon. *47th Lunar and Planetary Science Conference*. LPI Contribution No. 1903, p. 1238.

Gomes, R., Levison, H. F., Tsiganis, K., & Morbidelli, A. (2005). Origin of the Cataclysmic Late Heavy Bombardment of the Terrestrial Planets. *Nature*, 453, pp. 466-469.

Grinspoon, D. H. (1989). *Large impact events and atmospheric evolution on the terrestrial planets*. University of Arizona.

Hady, G. G., Abigail, C. D., Sebastian, H., Nicola, D. Q., Andrea, A., & Damian, B. (2016). ALCIDES: A novel lunar mission concept study for the demonstration of enabling technologies in deep-space exploration and human-robots interaction. *Proceedings of the International Astronautical Congress, IAC*, *October*.

Harrison, T. M., Hodges, K. V, Boehnke, P., Mercer, C. M., & Parisi, A. (2018). Problematic evidence of a Late Heavy Bombardment. *Bombardment: Shaping Planetary Surfaces and Their Environments 2018*.

Hartmann, W. K. (1975). Lunar “Cataclysm”: A Misconception ? *Icarus*, *24*, 181–187.

Hartmann, W. K. (2019). History of the terminal cataclysm paradigm: Epistemology of a planetary bombardment that never (?) happened. Geosciences (Switzerland), 9(7). https://doi.org/10.3390/geosciences9070285.

Hartung, J. B. (1974). Can random impacts cause the observed Ar 39/40 age distribution for lunar highland rocks? In *Meteoritics* (Vol. 9, p. 349).

Izidoro, A., Deienno, R., Raymond, S. N., & Clement, M. S. (2024). *Implantation of asteroids from the terrestrial planet region: The effect of the timing of the giant planet instability*. *15*, 0–3. http://arxiv.org/abs/2404.10831.

Kamata, S., Sugita, S., Abe, Y., Ishihara, Y., Harada, Y., Morota, T., Namiki, N., Iwata, T., Hanada, H., Araki, H., Matsumoto, K., Tajika, E., Kuramoto, K., & Nimmo, F. (2015). The relative timing of Lunar Magma Ocean solidification and the Late Heavy Bombardment inferred from highly degraded impact basin structures. *Icarus*, *250*, 492–503. https://doi.org/10.1016/j.icarus.2014.12.025.

Kring, D. A., & Cohen, B. A. (2002). Cataclysmic bombardment throughout the inner solar system 3.9-4.0 Ga. *Journal of Geophysical Research E: Planets*, *107*(2). https://doi.org/10.1029/2001je001529.

Lisse, C. M., Wyatt, M. C., Chen, C. H., Morlok, A., Watson, D. M., Manoj, P., Sheehan, P., Currie, T. M., Thebault, P., & Sitko, M. L. (2012). Spitzer evidence for a late-heavy bombardment and the formation of ureilites in η corvi at 1 Gyr. *Astrophysical Journal*, *747*(2), 1–60. https://doi.org/10.1088/0004-637X/747/2/93.

Lisse, C. M., Sitko, M. L., & Marengo, M. (2016). KIC 8462852: Further evidence for Late Heavy Bombardments in the astronomical record. *47th Lunar and Planetary Science Conference*.

Liu, T., Michael, G., & Wünnemann, K. (2023). The Timeline of Early Lunar Bombardment Constrained by the Evolving Distributions of Differently Aged Melt.

Planetary Science Journal, 4(7), 133. https://doi.org/10.3847/PSJ/ace0bb.

Lowe, D. R., & Byerly, G. R. (2018). The terrestrial record of Late Heavy Bombardment. In *New Astronomy Reviews* (Vol. 81, pp. 39–61). Elsevier B.V. https://doi.org/10.1016/j.newar.2018.03.002.

McDowell, J. (2007). *Lunar Nomenclature*. http://www.planet4589.org/astro/lunar.

Melosh, H. J. (1989). *Impact Cratering. A Geologic Process.* Clarendon Press.

Morbidelli, A., Marchi, S., Bottke, W. F., & Kring, D. A. (2012). A sawtooth-like timeline for the first billion years of lunar bombardment. *Earth and Planetary Science Letters*, *355–356*, 144–151. https://doi.org/10.1016/j.epsl.2012.07.037.

Morbidelli, A., Nesvorny, D., Laurenz, V., Marchi, S., Rubie, D. C., Elkins-Tanton, L., Wieczorek, M., & Jacobson, S. (2018). The timeline of the lunar bombardment: Revisited. *Icarus*, *305*, 262–276. https://doi.org/10.1016/j.icarus.2017.12.046.

Mordasini, C., & Burn, R. (2024). Planet formation -- observational constraints, physical processes, and compositional patterns. http://arxiv.org/abs/2404.15555

Neukum, G., Ivanov, B. A., & Hartmann, W. K. (2001). Cratering records in the inner solar system in relation to the lunar reference system. *Space Science Reviews*, *96*(1–4), 55–86. https://doi.org/10.1023/A:1011989004263.

Nesvorný, D., Roig, F. V., Vokrouhlický, D., Bottke, W. F., Marchi, S., Morbidelli, A., & Deienno, R. (2023). Early bombardment of the moon: Connecting the lunar crater record to the terrestrial planet formation. *Icarus*, 399, 1–75. https://doi.org/10.1016/j.icarus.2023.115545.

Raymond, S. N. (2024). The Solar System: structural overview, origins and evolution. 1–17. http://arxiv.org/abs/2404.14982.

Schmedemann, N., Kneissl, T., Ivanov, B.A., Michael, G.G., Wagner, R.J., Neukum, G., Ruesch, O., Hiesinger, H., Krohn, K., Roatsch, T., Preusker, F., Sierks, H., Jaumann, R., Reddy, V., Nathues, A., Walter, S.H.G., Neesemann, A., Raymond, C.A., & Rusell, C. T. (2014). The cratering record, chronology and surface ages of (4) Vesta in comparison to smaller asteroids and the ages of HED meteorites. *Planetary and Space Science* 103, 104-130. https://doi.org/10.1016/j.pss.2014.04.004.

Singh, T., Srivastava, N., Bhatt, M., & Bhardwaj, A. (2022). Geology of the Crüger-Sirsalis Basin: Evidence for prolonged volcanism in the southwestern near side of the Moon. *Icarus*, *376*(January), 114875. https://doi.org/10.1016/j.icarus.2021.114875.

Stöffler, D. & Ryder, G. (2001). Stratigraphy and isotope ages of lunar geologic units: Chronological standard for the inner solar system. *Space Science Reviews*, *96*(1–4), 9-54.

Tera, F., Papanastassiou, D. A., & Wasserburg, G. J. (1974). Isotopic evidence for a Terminal Lunar Cataclysm. *Earth and Planetary Science Letters*, *22*, 1–21. http://www.sciencedirect.com/science/article/pii/0012821X74900594.

The pandas development team. pandas-dev/pandas: Pandas, (February 2020). URL https://doi.org/10.5281/zenodo.3509134.

USGS Astrogeology Science Center, & International Astronomical Union. (n.d.). *Gazetteer of Planetary Nomenclature*. https://planetarynames.wr.usgs.gov.

Von Hegner, I. (2023). A potential survival strategy during the late heavy bombardment. *Serbian Astronomical Journal*, 206, 9–27. https://doi.org/10.2298/saj2306009h.

Walton, C. R., Jeon, H., Černok, A., Rae, A. S. P., Baziotis, I., Tang, F., Kuppili, V. S. C., Ferrière, L., Darling, J., Hu, S., Whitehouse, M. J., Anand, M., & Shorttle, O. (2023). In-situ phosphate U-Pb ages of the L chondrites. *Geochimica et*

Cosmochimica Acta, *359*(July), 191–204. https://doi.org/10.1016/j.gca.2023.07.012.

Wetherill, G. W. (1975). Late Heavy Bombardment of the Moon and Terrestrial Planets. *Proceedings of the Lunar Science Conference*, *6*, 1539–1561. http://adsabs.harvard.edu/abs/1975LPSC....6.1539W.

White, L. F., Moser, D. E., Darling, J. R., Rider-Stokes, B. G., Hyde, B., Tait, K. T., Chamberlain, K., Schmitt, A. K., Dunlop, J., & Anand, M. (2024). Accessory mineral microstructure and chronology reveals no evidence for late heavy bombardment on the asteroid 4-Vesta. *Earth and Planetary Science Letters*, *636*(March), 118694. https://doi.org/10.1016/j.epsl.2024.118694.

Wilhelms, D. E., McCauley, J. F., & Trask, N. J. (1987). *The Geologic History of the Moon*. United States Geological Surver.

Worsham, E. A., & Kleine, T. (2020). Constraining the Late Heavy Bombardment of the Moon using Ru isotopes in lunar impactites. *51st Lunar and Planetary Science Conference*.

Worsham, E. A., & Kleine, T. (2021). Late accretionary history of Earth and Moon preserved in lunar impactites. In *Sci. Adv* (Vol. 7). https://www.science.org.

Xie, M., Xiao, Z., Xu, L., Fa, W. and Xu, A. (2021). Change in the Earth-Moon impactor population at about 3.5 billion years ago. *Nature astronomy*, 5, pp. 128-133.

Zellner, N. E. B. (2017). Cataclysm no more: New views on the timing and delivery of lunar impactors. *Orig. Life Evol. Biosph.*, 47, pp. 261-280.

Zhao, C., Yue, Z., Di, K., Jia, Y., Ip, W. H., Lin, Y., Wu, B., Wang, B., & Xie, B. (2024). Asymmetrical distribution of 1–20 km craters on the Moon. *Planetary and Space Science*, *254*. https://doi.org/10.1016/j.pss.2024.106015.